Research on Chemical Intermediates
https://doi.org/10.1007/s11164-024-05322-5

Insights into the promising heterogeneous catalysis of eco-friendly synthesized spinel $CuFe_2O_4$ nanoparticles for Biginelli reaction

Dnyaneshwar Sanap[1,2] · Lata Avhad[3] · Satish Ahire[4] · Mahmoud Mirzaei[5] · Deepak Kumar[6] · Suresh Ghotekar[7] · Nitin D. Gaikwad[1]

Received: 31 March 2024 / Accepted: 1 June 2024

Abstract

Spinel copper ferrite magnetic nanoparticles ($CuFe_2O_4$ MNPs) are one of the prominent spinel ferrites due to their magnetic properties. As a result of the current investigation, the magnetic spinel copper ferrite nanoparticles ($CuFe_2O_4$ MNPs) were successfully fabricated via a green synthesis approach using freshly prepared Yogurt of cow milk as a capping agent by sol–gel auto-combustion route and its catalytic effect towards synthesizing ethyl 1,2,3,4-tetrahydro-2-oxo-4-aryl pyrimidine-5-carboxylate (DHPMs) scaffold was explored. Further, the phase formation, crystallinity, particle size, grain morphology, and the property of magnetism of bio-fabricated spinel $CuFe_2O_4$ NPs were explored by XRD, FESEM, EDX, FTIR, UVDRS, and VSM analysis. Furthermore, one-pot synthesis of DHPMs scaffold via multicomponent (MCR) Biginelli reaction was examined using biosynthesized spinel $CuFe_2O_4$ magnetic heterogeneous catalyst (C1 and C2 nanocrystalline phase). To achieve the high yields (90–98%) of DHPMs scaffold synthesis with an extensive range of aromatic carbaldehyde using minimum loading of heterogeneous catalysts within minimum reaction time and easy catalyst recovery by a peripheral magnet were examined. Therefore, this protocol presents an extensive scope for Biginelli reaction using magnetically separable heterogeneous catalyst synthesis via a green approach.

Extended author information available on the last page of the article

Published online: 16 June 2024

Graphical abstract

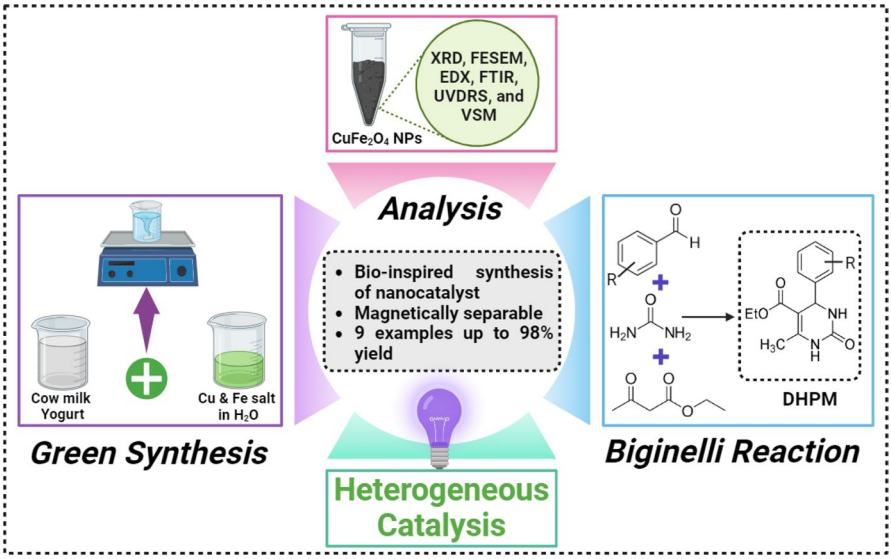

Keywords Green synthesis · $CuFe_2O_4$ NPs · Heterogeneous nanocatalysis · Magnetically retrievable catalyst

Introduction

Modern nanotechnology has proliferated rapidly due to nanomaterial's wide range of structural, geometrical, and molecular functionalities [1–3]. The lesser the nanoparticle size, the more active sites there are on a nanoparticle's surface per unit surface, which is relevant to the disciplines of electronics, sensors, energy, biology, and catalysts [4–12]. Spinel ferrites are often studied because of their usefulness and peculiar features [13]. Spinel copper ferrite is the most popular magnetic material; therefore, it can be used in energy storage [14], biomedicine [15], sensors [16], photocatalyst [17, 18], as a magnetic material [19], and heterogeneous catalyst for organic transformation [20–23]. Several methods are reported for synthesizing spinel $CuFe_2O_4$ nanomaterials, such as co-precipitation [24], hydrothermal [25–27], and sol–gel [25]. However, these methods have their limitation, such as toxicity, non-eco-friendly, and environmentally friendly [28]. To overcome these challenges, the green synthesis of nanomaterials using natural resources as a bio-reductant has played an efficient, innocuous, and ecologically friendly synthesis route [29–31]. In the literature, copper ferrite was successfully synthesized using a green method using aqueous extracts of various plant parts [32], waste eggshells [33, 34], and cow urine [35]. Therefore, in this work, we synthesized spinel copper ferrite

nanoparticles using freshly prepared cow milk yogurt, which had yet to be reported. It is environmentally friendly, cost-effective, and non-toxic.

Because yogurt has a high amount of residing lactic acid bacteria, which compete with various opportunistic microorganisms and produce beneficial metabolites that support consumer health as well as the production of yogurt flavor and scent, yogurt is a rich source of health-promoting nutrients [36]. Yogurt can be prepared to utilize milk from several species. Yogurt features like flavor, price, and convenience also play a significant role in determining how well-liked the end product is by consumers. Cow milk was frequently used in earlier dairy science investigations, possibly due to their high volume and significance to the economy. Studies have shown that biologically active substances and minerals such as calcium, phosphorus, potassium, sodium, lactose, galactose, thiamine, riboflavin, acetic acid, lactic acid, glucose., are present in cow yogurt (Fig. 1) [37, 38].

Formerly, $CuFe_2O_4$ nanoparticles were used as a heterogeneous catalyst in organic transformation via Spiro pyrazole derivative synthesis [39], imidazole derivative synthesis [22, 40], quinolines derivative synthesis [41], and in Mannich reaction to produce β-amino carbonyl compounds via MCRs [42]. Herein, due to their crucial role in medicines, we effectively report the preparation of DHPMs derivatives using bio-fabricate $CuFe_2O_4$ MNPs (Scheme 1).

The DHPMs and their scaffolds are found in nature and marine sources. They have widespread attention due to their pharmaceutical and therapeutic properties in anticancer [43], antifungal [44], anti-inflammatory [45], antibacterial [46], antidiabetics [47], antithyroid [48], anti-neoplastic [49], Alzheimer's ailment [50], and neuro disorders [49].

Traditionally, DHPMs and scaffolds were synthesized in homogeneous conditions using the protic solvent or acid catalyst [51, 52] and Lewis acid

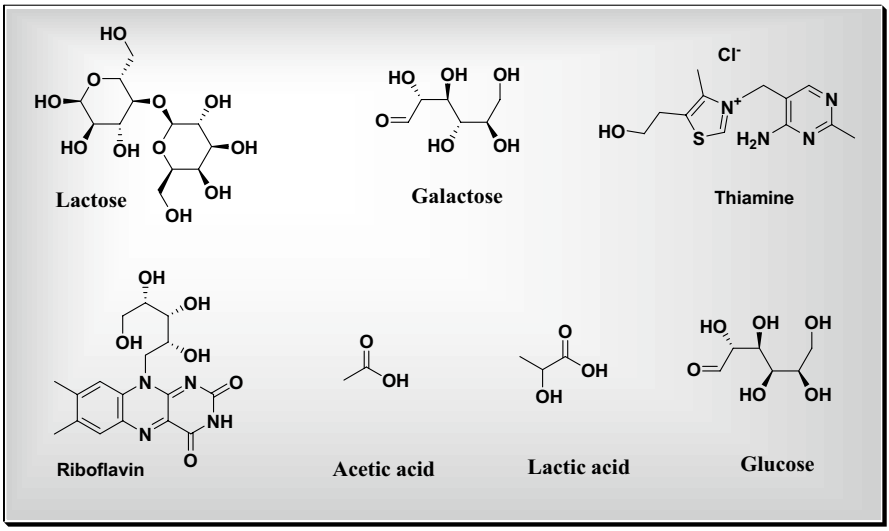

Fig. 1 Biomolecules present in cow milk yogurt

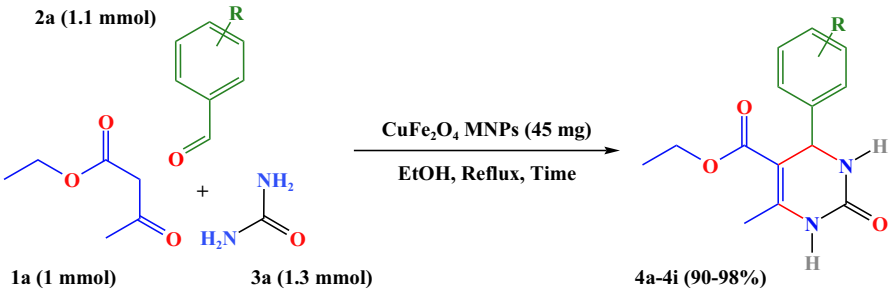

Scheme 1 Strategy for the building of DHPMs derivative

catalyst [53, 54]. Paraskar et al. [53] report the Lewis acid catalyzed preparation of 3,4-dihydropyrimidine-2(1H)-ones (Yield 60–95%) employing $Cu(OTf)_2$ as a reusable catalyst for five successive cycles in the presence of acetonitrile as a solvent for 6 to 12 h. K. Ananda Kumar et al. [54] reports Lewis acid-catalyzed preparation of 4-aryl 3,4-dihydropyrimidine-2-ones (Yield 75–96%) utilizing a catalytic amount of manganeses(III) acetate under refluxing condition in presence of acetonitrile as a medium for 2 to 4 h. Ichiro Suzuki et al. [55] successfully report the Biginelli reaction (Yield 25–88%) using metal triflimide ($Yb(NTf_2)_2$, $Ni(NTf_2)_2$, and $Cu(NTf_2)_2$,) as Lewis acid catalyst in aqueous medium for 72 h. Zhao et al. [56] investigated the Biginelli synthesis (Yield 88–93%) using single-site Lewis and Bronsted acid in a metal–organic framework (Ni-DDIA) under N_2 atmospheric conditions for 30 min. However, other heterogeneous catalysts have been reported for organic transformations [57–59].

In the last decades, heterogeneously catalyzed DHPMs and scaffold synthesis were reported using metal oxide, mixed metal oxide [60], nanocomposite [61, 62], and magnetic nanomaterial [63]. In 2013, Safari et al. [61] described the microwave-assisted (MW 80 w) solvent-free Biginelli synthesis (Yield 87–97%) using MnO_2-CNT nanocomposite for substituted aldehyde and ketones within 5 to 25 min. Javad Safaei Ghomi et al. [62] report the green preparation of 3,4-dihydropyrimidine-2(1H)-one or Thion scaffold (Yield 68–97%) synthesis applying nano-silica-supported tin(II) chloride as heterogeneous nanocatalyst for substituted aromatic aldehyde within 35–48 min in the presence of ethanol as a solvent. In 2018, Shanmugam Prakash et al. [64] demonstrated the Biginelli synthesis (Yield 87–98% within 50–120 min) catalyzed by CuO NPs as a novel heterogeneous catalyst fabricated by a green approach using *Cordia sebestena (C. sebestena)* flowers aqueous extract. Zamani et al. [65] explored the solvent-free Biginelli synthesis (Yield 75–92% within 115–185 min) using Fe_3O_4 nanoparticles coated by sulfonated-phenylacetic acid as a novel acidic magnetic catalyst at room temperature. Girija et al. [66] report the solvent-free microwave-assisted (MW 200 w) preparation of 3,4-dihydropyrimidine-2(1H)-one (Yield 86–90 within 5–8 Min) using magnetically separable Fe_3O_4-bpy-Ni(II) complex as a heterogeneous catalyst at 130 °C. Chaudhary et al. [67] explored the

solvent-free microwave-assisted (MW 800 w) Biginelli synthesis (Yield 86–97% within 1.5–3 min) using recyclable CuS quantum dots as a novel heterogeneous catalyst.

However, around six challenges are entrenched in preparing DHPMs derivative: (1) Using a potentially dangerous homogeneous catalyst; (2) Using a potentially harmful reagents; (3) Inadequate yield; (4) Requirement of too much time for reaction completion; (5) Difficult to reaction workup; (6) Difficulties in the retrieval of catalysts.

Therefore, there is a comprehensive scope to develop a synthetic methodology for the quick synthesis of DHPMs scaffold to achieve experimental beneficence, simplicity, sustainability, and reaction efficacy. To overcome these challenges, we developed the successful synthesis of DHPMs derivatives using a heterogeneous magnetic catalyst synthesized by a green approach, with a yield in the range of 90–98%. Moreover, the structure of the produced derivative of the Biginelli reaction has also been validated by ^{1}H and ^{13}C NMR.

Experimental

Materials

Cow milk, Lemon fruit, Yogurt, ferric chloride hexahydrate ($FeCl_3$ $6H_2O$), copper chloride dihydrate ($CuCl_2$ $2H_2O$), substituted aromatic aldehydes, n-hexane, ethyl alcohol, and ethyl acetate were acquired from S.D. Fine Chemical Limited. All solvents were distilled before being employed in this experiment.

Preparation of fresh Yogurt

In a 250 mL beaker, 130 mL of fresh cow milk was well mixed with 5 mL of Lemon fruit juice and kept for the next 24 h in the dark to make Yogurt (commonly fermented milk, i.e., Dahi in Marathi regional language). After that, water was removed by decanting the solution to free the Yogurt from excess water.

Synthesis of spinel $CuFe_2O_4$ MNPs

A simple sol–gel auto-combustion process was used for the successful bio-fabrication of spinel $CuFe_2O_4$ MNPs using the 1:2 mixture of $CuCl_2.2H_2O$ and $FeCl_3.6H_2O$ in the presence of yogurt as a fuel that serves as a good platform for redox reactions to occur during auto-combustion.

In a 250 mL beaker, 100 mL of freshly prepared Yogurt of cow milk was taken and stirred for 1 h at 200 rpm to make a homogeneous mixture. At the same time, the 15 mL homogeneous salt solution of $CuCl_2.2H_2O$ and $FeCl_3.6H_2O$ was prepared by dissolving the 2.13 g of $CuCl_2.2H_2O$ and 6.75 g $FeCl_3.6H_2O$ in tripled distilled water with constant stirring for the 30 min, the same homogeneous salt solution was drop by drop added to Yogurt solution at RT over the 30 min. Ensuring the

addition of salt solution was over, the solution was stirred for 2 h. After that, the thick paste was obtained by heating the subsequent mixture on the hot plate at 70–80 °C for 2 h, followed by a thick mass by retaining the paste in a hot air oven at 100–120 °C for 5 h for auto-combustion. Finally, dry powder was obtained after grinding the thick mass in a mortar pestle for 30 min [29]. For 3 h, the dry $CuFe_2O_4$ powder was calcined at 600 and 750 °C temperatures separately and obtained the dark reddish brown and dark black $CuFe_2O_4$ materials, which were labeled as C1 ($CuFe_2O_4$ calcined at 600 °C) and C2 ($CuFe_2O_4$ calcined at 750 °C), respectively. A typical bio-inspired synthetic route for producing $CuFe_2O_4$ MNPs is shown in Fig. 2. Finally, the synthesis of DHPMs derivatives was screened using C1 and C2 nanocrystalline spinel $CuFe_2O_4$ MNPs.

Catalytic study: general procedure for Biginelli multicomponent cycloaddition reaction to produce DHPMs scaffold

In a 25 mL round bottom flask, in combination with just distilled 1 mmol ethyl acetoacetate, the 1.1 mmol substituted aromatic carbaldehyde, 1.3 mmol urea, 0.019 mmol; 8.15 mol % biosynthesized (C1) $CuFe_2O_4$ MNPs and ethanol (5 mL) was well refluxed (Scheme 2). TLC was performed using ethyl acetate and n-hexane in a 1:1 proportion to monitor the reaction progress of DHPMs scaffold synthesis. Once the reaction had finished, the liquid supernatant layer of ethanol was decanted via Whatman filter paper by keeping the RB near the external magnet to separate the

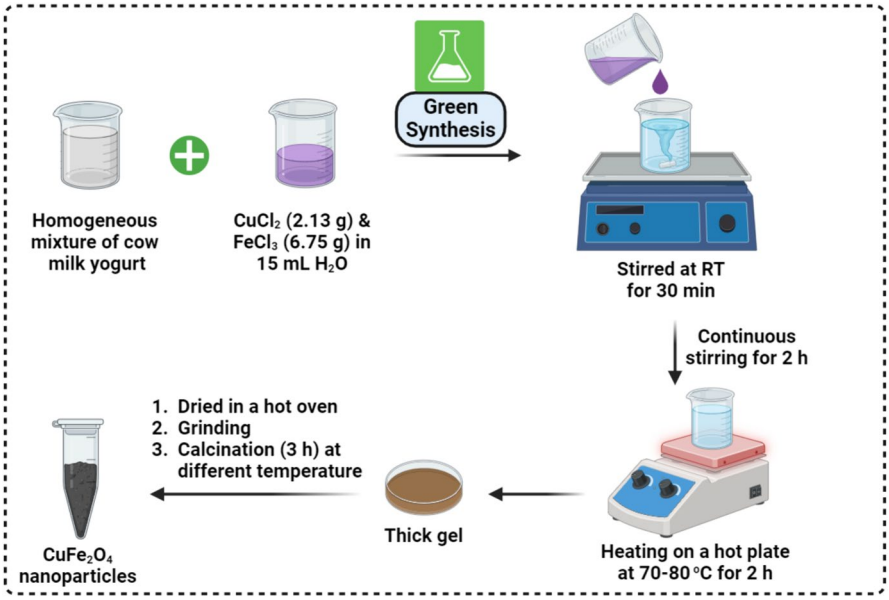

Fig. 2 A schematic illustration of the $CuFe_2O_4$ MNPs production via cow milk yogurt (biorender.com)

spinel $CuFe_2O_4$ catalyst. The purified product was confirmed by ^1H and ^{13}C NMR techniques.

Characterization techniques

The phase formation and crystal structure of biosynthesized $CuFe_2O_4$ MNPs was confirmed using a Bruker D8 diffractometer having 1.54060 A^0 Cu-K radiation, angle 20–80°, with a 0.020° step size of 2θ. The surface structure, cross-section morphology, element mapping, and percent element composition of synthesized spinel MNPs were examined using the FEI Nova Nano SEM 450 instrument with a 10 kV as an accelerating voltage. The FTIR analysis of spinel MNPs in the 400 to 4000 cm^{-1} range was carried out using a Type-A, JASCO-4600 spectrophotometer. A UV-DRS of biosynthesized $CuFe_2O_4$ MNPs was measured using a Jasco Spectrophotometer Model V-770 in the 200 to 800 nm range. The magnetic behavior of biosynthesized NPs was analyzed using VSM. The physical constant (Melting Point) of the synthesized DHPMs scaffold was measured using Thiele's tube assembly. Finally, the molecular structure of the produced DHPMs derivatives was validated using the Bruker Advance 500 MHz Spectrometer, which has an instrument strength of 500 and 126 MHz for ^1H and ^{13}C nuclei, respectively.

Spectral data of synthesized compounds

This is compiled in the electronic supplementary material data file.

Results and discussion

XRD analysis

The crystallographic structure and phase formation of biosynthesized $CuFe_2O_4$ MNPs (C1, C2) were explored using XRD measurement Fig. 3. The typical diffraction peaks of $CuFe_2O_4$ MNPs found at 2θ: 29.92, 30.76, 34.56, 36.09, 37.20, 41.44, 44.13, 54.22, 55.02, 57.15, 58.22, 62.14, 64.10, 74.80, 76.50, and 79.28° with the miller indices of (112), (200), (013), (211), (202), (004), (220), (312), (015), (303), (321), (224), (400), (413), (422), and (404). The indexing pattern of synthesized $CuFe_2O_4$ MNPs (C1, C2) according to $CuFe_2O_4$ MNPs standard diffraction pattern data with the tetragonal spinel-l41/amd space group. This outcome is sufficiently consistent with the earlier research [68]. However, some diffraction peaks shown by asterisk mark (*) in XRD indicate an unidentified impurity phase formation during the $CuFe_2O_4$ MNPs (C1, C2) synthesis. The mean crystalline size of biosynthesized $CuFe_2O_4$ MNPs (C1, C2) was calculated by the FWHM value of all the peaks using the Scherer equation, and it has come across to be 14.64 and 25.21 nm for C1 and C2 samples, respectively (Table 1).

Scheme 2 Spinel $CuFe_2O_4$ (C1) catalyzed synthesis of ethyl 1,2,3,4-tetrahydro-6-methyl-2-oxo-4-aryl ▶ pyrimidine-5-carboxylate derivative (4a-4i) using ethyl acetoacetate (1a) with aromatic carbaldehyde (2a-2i) and Urea (3a)

FESEM study

Furthermore, the grain surface morphology and element mapping of bio-fabricated $CuFe_2O_4$ MNPs (C1, C2) were investigated using FESEM analysis (Fig. 4). It can be seen that $CuFe_2O_4$ MNPs show spherical and sheet, octahedral (mixed shapes) shapes for C1 (Fig. 4a–b) and C2 (Fig. 4e–f) samples, respectively. The elemental mapping was carried out to find out the distribution of Cu (Copper), Fe (Iron), and Oxygen (O) elements in biosynthesized C1 (Fig. 4c–d) and C2 (Fig. 4g–h) $CuFe_2O_4$ MNPs, respectively.

EDX study

Additionally, the elemental composition of biosynthesized $CuFe_2O_4$ MNPs was analyzed by EDX analysis (Fig. 5). The EDX pattern indicates and confirms the presence of Copper (Cu), Iron (Fe), and Oxygen (O) elements in the C1 (Fig. 5a) and C2 (Fig. 5b) samples, which confirms the successful synthesis of $CuFe_2O_4$ MNPs (Fig. 5c).

FTIR analysis

The chemical bonding nature in the biosynthesized $CuFe_2O_4$ MNPs was investigated using FTIR (Fig. 6). The spectrum of as-biosynthesized spinel $CuFe_2O_4$ MNPs shows prominent peaks at 540, 1042, and 1589 cm^{-1}. The vibration in the range of 100 to 1000 cm^{-1} corresponds to the metal oxide $CuFe_2O_4$ MNPs' absorbance at tetrahedral sites [69]. The 1589 and 1042 cm^{-1} peaks may resemble the bending and stretching vibration of amide N–H bonds, aromatic C=C bonds, and aliphatic ether C–O bonds, respectively. Peaks at 540 cm^{-1} related to Cu–O and Fe–O bonds in $CuFe_2O_4$ (C1 and C2) samples [19, 70].

UV-DRS study

Additionally, the light absorbance properties of bio-fabricated spinel C1 and C2 $CuFe_2O_4$ MNPs were explored in the range of 200 to 800 nm. Samples C1 and C2 show strong absorbance in the 200 to 650 nm region (Fig. 7a). Furthermore, the bandgap energy of bio-fabricated $CuFe_2O_4$ MNPs was estimated by direct method Tauc's plot and was found to be 1.67 and 1.49 eV for C1 and C2 samples (Fig. 7b).

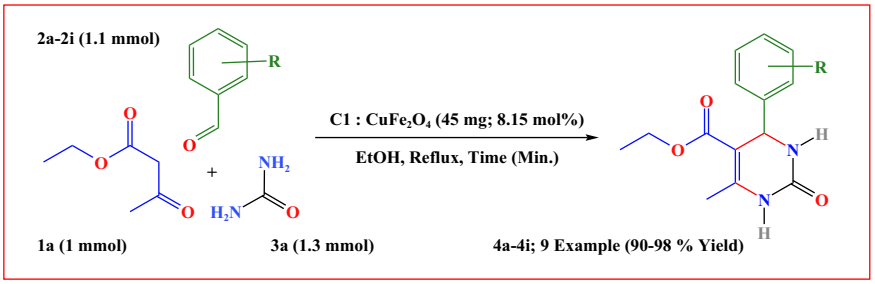

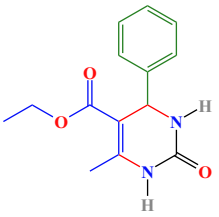
4a (40 Min, 98%)

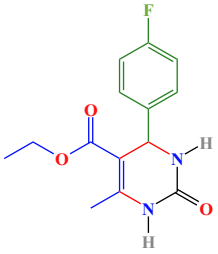

4b (40 Min, 97%)

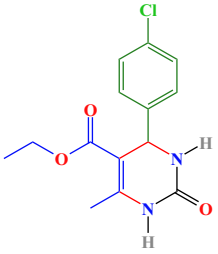

4c (40 Min, 98%)

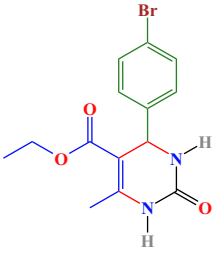

4d (40 Min, 97%)

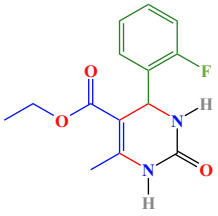

4e (50 Min, 95%)

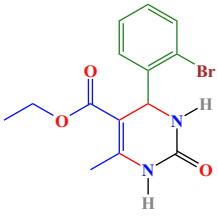

4f (50 Min, 92%)

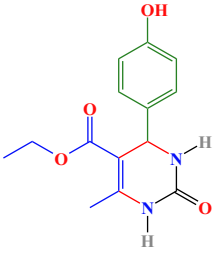

4g (40 Min, 93%)

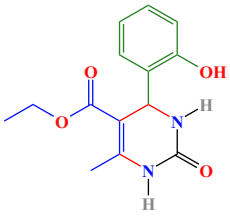

4h (50 Min, 91%)

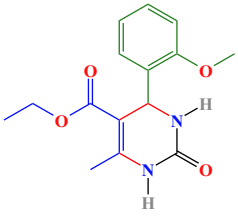

4i (50 Min, 90%)

Reaction Condition: Ethyl acetoacetate (1 mmol), Aromatic aldehyde (1.1 mmol), Urea (1.3 mmol), Ethanol (5 ml), (C1)-$CuFe_2O_4$ MNPs (45 mg; 8.15 mol%) under reflux condition. Time required for reaction and Isolated yield shown in parenthesis.

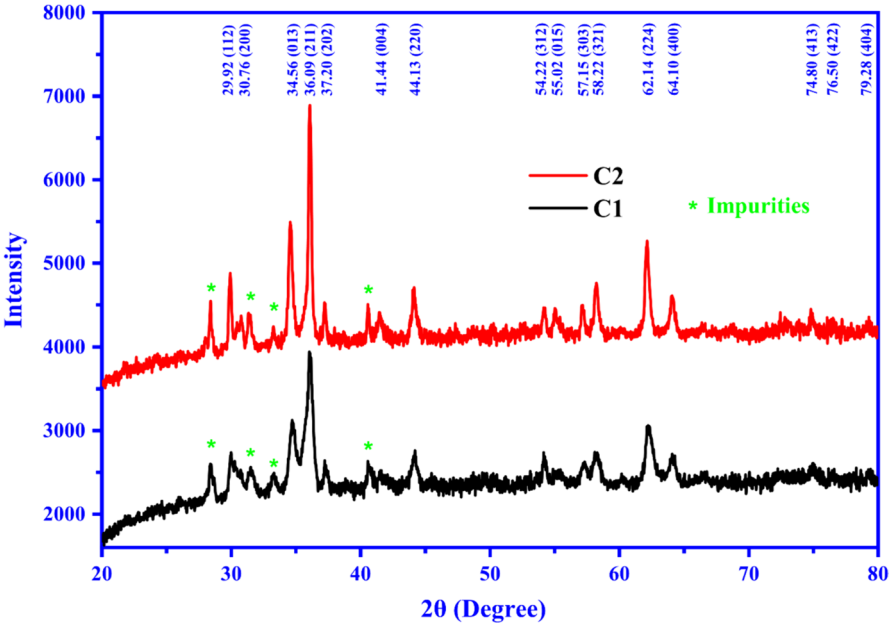

Fig. 3 XRD of spinel $CuFe_2O_4$ MNPs; Calcined at 600 °C (C1), and 750 °C (C2)

Table 1 The mean crystal size of green synthesized spinel $CuFe_2O_4$ MNPs by Scherer equation based on FWHM for some prominent peaks

Name of the sample with code	2θ	F.W.H.M	Grain size D (nm)	Mean size (D)
$CuFe_2O_4$ MNPs (C1)	34.56	0.8269	09.84	14.64 nm
	36.09	0.7243	11.28	
	37.20	0.4794	17.10	
	44.13	0.5436	15.42	
	58.22	0.5308	16.75	
	62.14	0.6303	14.40	
	64.10	0.5190	17.66	
$CuFe_2O_4$ MNPs (C2)	29.92	0.2747	28.60	25.21 nm
	34.56	0.4060	19.58	
	36.09	0.3179	25.11	
	37.20	0.2392	33.48	
	44.13	0.3875	21.14	
	58.22	0.3377	25.73	
	62.14	0.3744	23.67	
	64.10	0.3671	24.39	

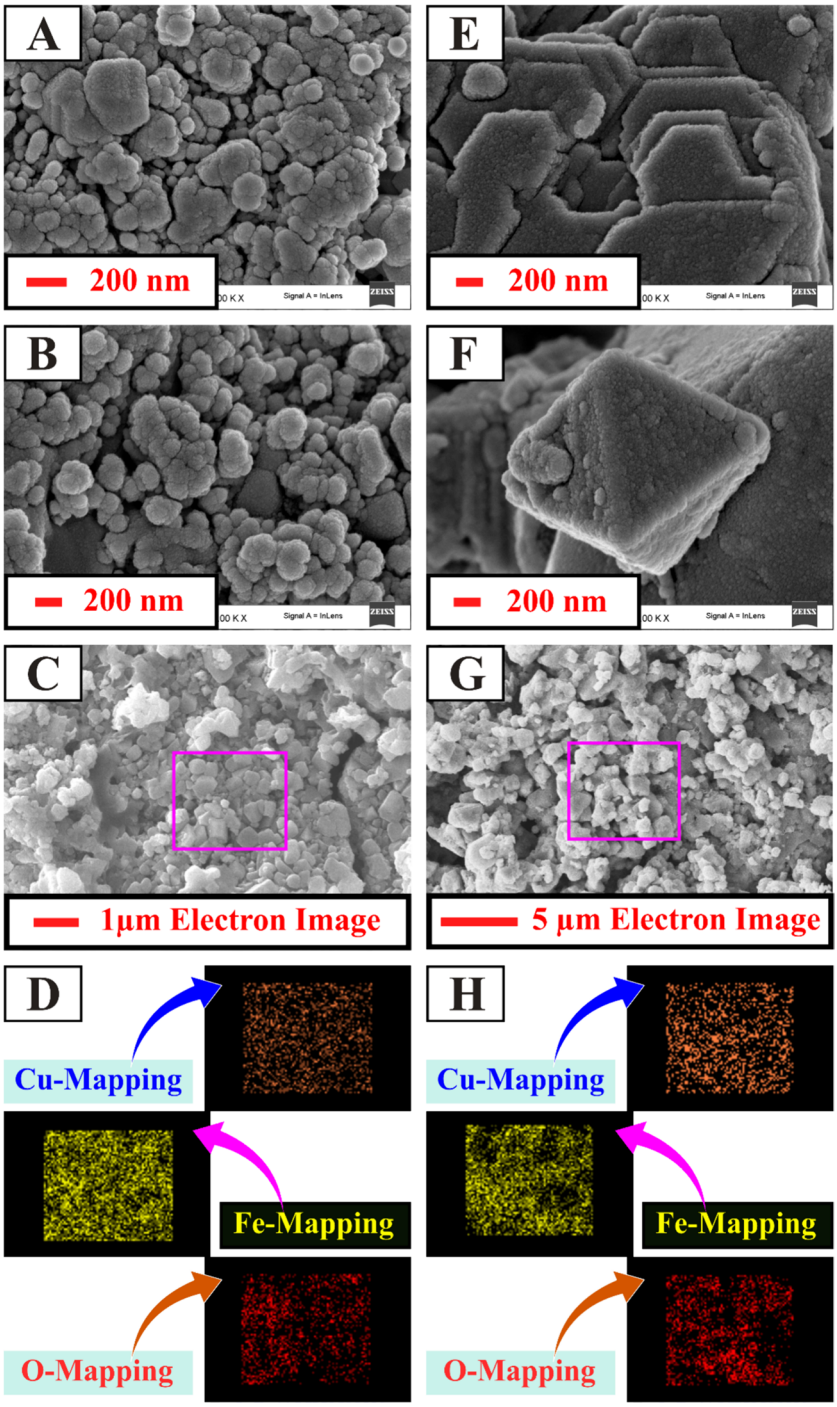

Fig. 4 FESEM images of as-biosynthesized spinel $CuFe_2O_4$ MNPs; C1 (**a**–**b**), and C2 (**e**–**f**); Element mapping of as-prepared MNPs C1 (**c**–**d**), and C2 (**g**–**h**)

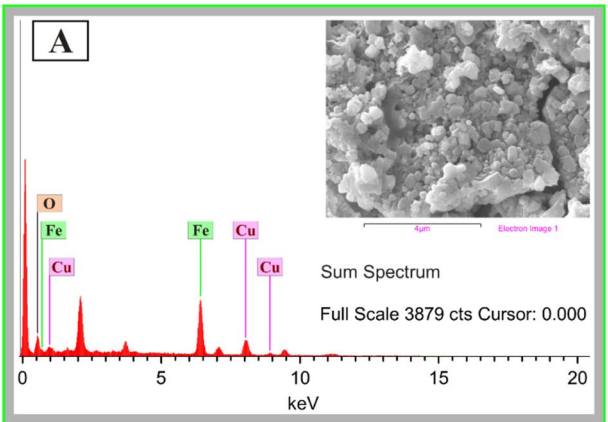

C

Sample	Element	Weight %	Atomic %
C1 ($CuFe_2O_4$)	Cu	29.07	18.33
	Fe	53.69	38.51
	O	17.24	43.17
C2 ($CuFe_2O_4$)	Cu	27.04	53.62
	Fe	48.00	30.67
	O	27.96	15.71

Fig. 5 EDX spectrum of biosynthesized C1, and C2 $CuFe_2O_4$ MNPs (**a**–**b**); element composition (%) of C1, and C2 $CuFe_2O_4$ MNPs (c)

VSM analysis

The magnetic features of bio-fabricated $CuFe_2O_4$ MNPs were studied by Vibrating

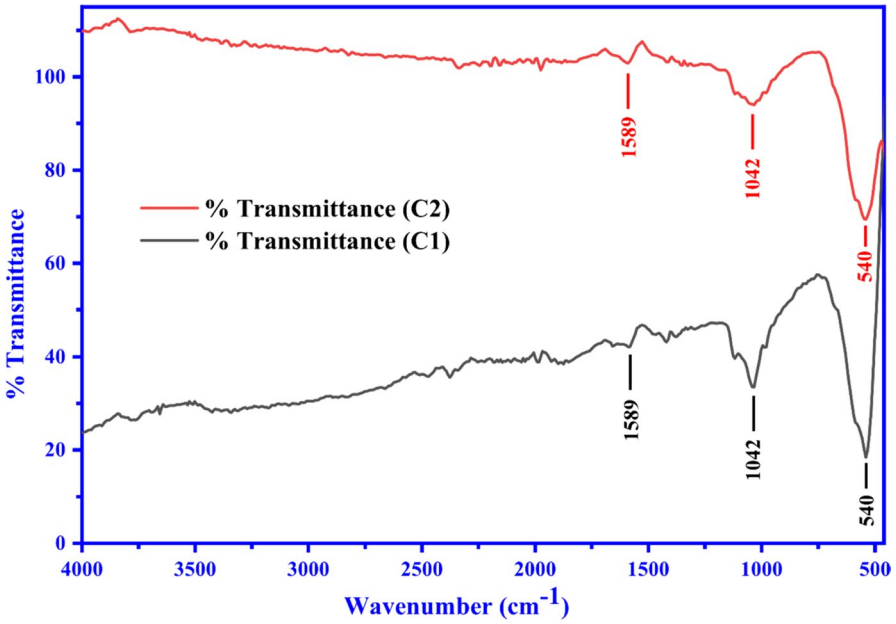

Fig. 6 FTIR spectra of biosynthesized spinel $CuFe_2O_4$ MNPs, Calcined at 600 °C (C1), and 750 °C (C2)

Sample Magnetometer (VSM) via a hysteresis loop between − 15 to 15 kOe range (Fig. 8) in the presence of a magnetic field. The value of magnetic field Coercivity (Hc), Saturation Magnetization (Ms), and Remnant Magnetization (Mr) was projected based on the M–H loop (Table 2). The magnetic nanomaterial is classified as a soft and hard ferromagnetic material based on coercivity, remanence, and saturation magnetization value. If the value of Hc and Mr is lower and Ms is higher, then the material is soft ferromagnetic and vice versa [69]. If the value of Hc is less than 50 Oe, the resulting nanomaterial is superparamagnetic [71]. Therefore, in comparison with various plant-part mediated and various fabrication approaches applied in previous studies (Table 3), the yogurt mediated biosynthesized $CuFe_2O_4$ MNPs are hard ferromagnetic materials indicated by the high value of Coercivity (Hc) and saturation magnetic magnetization (Ms). Therefore, the bio-fabricated $CuFe_2O_4$ NPs are helpful for easy separation from the reaction mixture at the end of the reaction by applying the external magnetic field using an ordinary permanent magnet.

Optimization of reaction condition for the synthesis of ethyl 1,2,3,4-tetrahydro-2-oxo-4-phenyl pyrimidine-5-carboxylate (4a)

In this study, we applied a heterogeneous spinel $CuFe_2O_4$ catalyst (C1 and C2) to synthesize ethyl 1,2,3,4-tetrahydro-2-oxo-4-phenyl pyrimidine-5-carboxylate derivatives from freshly distilled ethyl acetoacetate (1a), benzaldehyde (2a) and

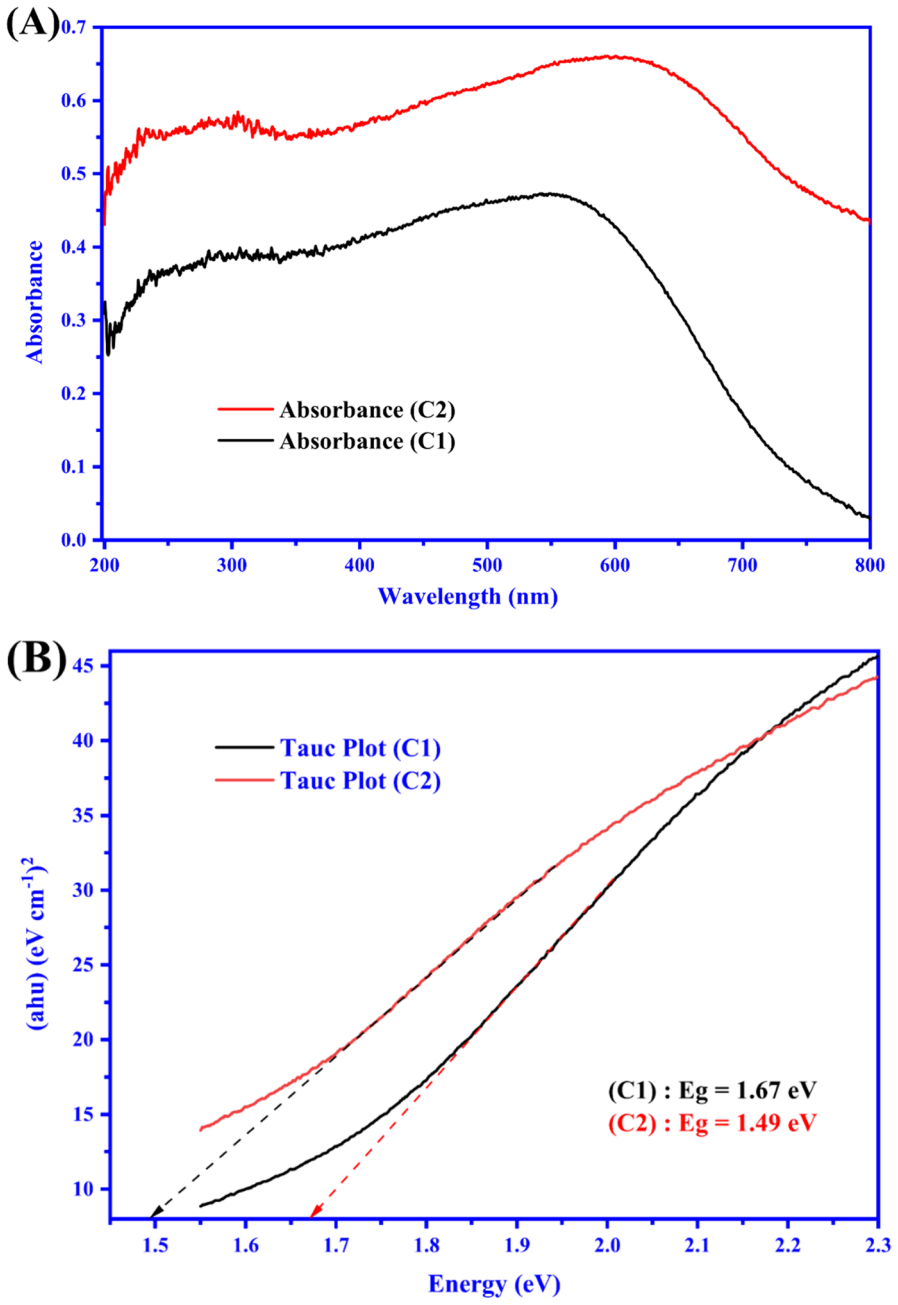

Fig. 7 **(a)** UVDRS spectra of bio-fabricated spinel C1, and C2 $CuFe_2O_4$ MNPs and (**b**) Tauc Plot (bandgap energy) for spinel C1, and C2 $CuFe_2O_4$ MNPs

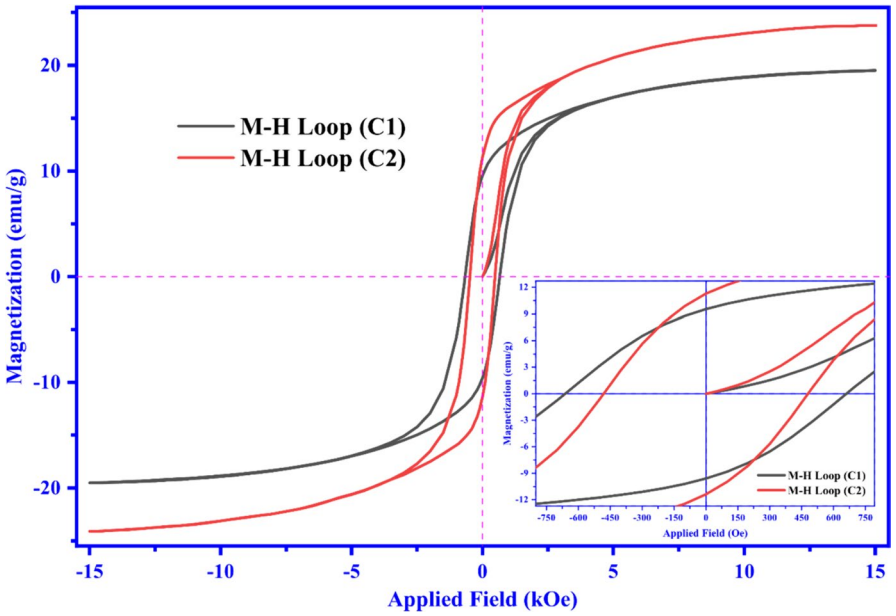

Fig. 8 Magnetization against applied field curve (M-H Loop) for C1, C2 spinel $CuFe_2O_4$ MNPs measured at room temperature

Table 2 Magnetic properties of biosynthesized spinel $CuFe_2O_4$ MNPs

Name of the sample with code	Coercivity (Hc) (Oe)	Saturation magnetization (Ms) (emu g^{-1})	Remnant field (Mr) (emu g^{-1})
$CuFe_2O_4$ MNPs (C1)	661.19	19.52	9.53
$CuFe_2O_4$ MNPs (C2)	481.12	23.78	11.25

dried urea (3a) to produce ethyl 1,2,3,4-tetrahydro-2-oxo-4-phenyl pyrimidine-5-carboxylate (4a) under refluxing conditions with ethyl alcohol (5 mL).

C1 and C2 spinel $CuFe_2O_4$ magnetic heterogeneous catalysts (15 mg; 2.87 mol%) were studied for the preparation of ethyl 1,2,3,4-tetrahydro-2-oxo-4-phenylpyrimidine-5-carboxylate derivatives by employing the 1 mmol of ethyl acetoacetate (1a) with 1.1 mmol benzaldehyde (2a) and 1.3 mmol urea (3a). The yields of 4a are summarised in Table 4 (Entry 1–9) when using C1 and C2 spinel $CuFe_2O_4$ heterogeneous catalysts.

In addition, the mole fractions of urea (3a) and benzaldehyde (2a) were optimized for the model synthesis of ethyl 1,2,3,4-tetrahydro-6-methyl-2-oxo-4-phenylpyrimidine-5-carboxylate derivatives for ethyl acetoacetate (1a; 1 mmol) utilizing C1 ($CuFe_2O_4$ MNPs; 15 mg; 2.87 mol %) as a potential catalyst for the Biginelli reaction. The reaction between 1.1 mmol of benzaldehyde and 1.3 mmol

Table 3 The features of spinel $CuFe_2O_4$ NPs fabricated by various methods

Capping agent	Method of synthesis	Morphology	Particle size (nm)	Saturation Magnetization (Ms) (emu g^{-1})	Coercivity (Hc) (Oe)	References
Cow-urine	Green synthesis	Spherical	14.5–22.3	10.2–35.4	0.72–3.35	[72]
Neem leaf extract and NaOH	Green synthesis	Spherical	19.7	NR	NR	[73]
Morus alba L. leaf extract	Green synthesis	Spherical	20–40	14.16	175.44	[42]
Yogurt	**Green synthesis**	**Spherical**	**14.64**	**19.52**	**661.19**	**Present work**
		Sheet like and Octahedral	**25.21**	**23.78**	**481.12**	

Table 4 Catalyst screening for the synthesis of ethyl 1,2,3,4-tetrahydro-6-methyl-2-oxo-4-phenylpyrimidine-5-carboxylate [a]

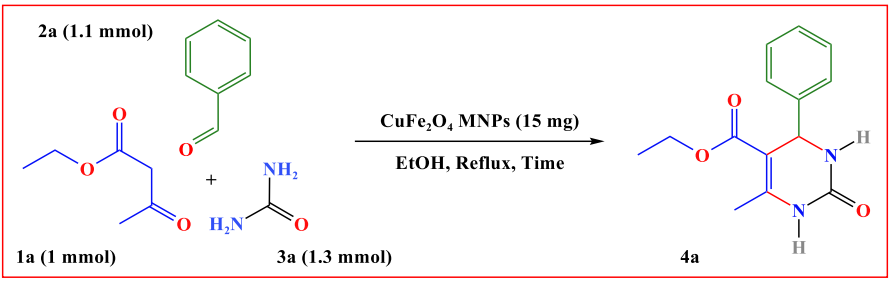

Entry	Used catalyst	Reaction time	Yield [b] (4a %)
1	–	30	Trace
2	C1	50	32
3	C2	50	19
4	C1	70	53
5	C2	70	40
6	**C1**	**90**	**77**
7	C2	90	64
8	C1	110	79
9	C2	110	63

[a]1.1 mmol Benzaldehyde, 1.3 mmol Urea, 1 mmol Ethyl acetoacetate, 5 mL Ethyl alcohol, C1/C2-Catalyst (15 mg; 2.87 mol %)

[b]Yield that can be isolated

The best values indicates in bold

of dried urea produced the greatest yield of 4a (77%) in ethyl alcohol after 90 min of refluxing (Table 5, Entry 5).

The maximum yield of 4a (98%) was obtained in 40 min for 45 mg (8.14 mol%) of catalyst when the catalytic quantity of $CuFe_2O_4$ (C1) was examined under optimal conditions- 1 mmol (1a), 1.1 mmol (2a), 1.3 mmol (3a), and ethanol (5 mL) as a medium (Table 6**,** Entry 7).

In heterogeneous catalysis, the catalytic performance of synthesized nanocatalysts depends on their effectiveness in catalyzing chemical reactions. In this work, the catalytic activity of a manufactured nanocatalyst was significantly influenced by its spherical, sheet, and octahedral morphology. A particular shape offers more active sites for the reaction and shows increased catalytic activity. Additionally, the components (Cu and Fe) of spinel $CuFe_2O_4$ showed synergistic effects, resulting from combining two distinct metals and improved catalytic performance. These metals improved the efficiency and selectivity of catalyzing reactions by stabilizing the crystal structure and creating active sites for the reaction. Moreover, spinel $CuFe_2O_4$ acts as Lewis acids to activate specific

Table 5 Investigation of urea and benzaldehyde mole fraction for the synthesis of ethyl 1,2,3,4-tetrahydro-6-methyl-2-oxo-4-phenylpyrimidine-5-carboxylate [a]

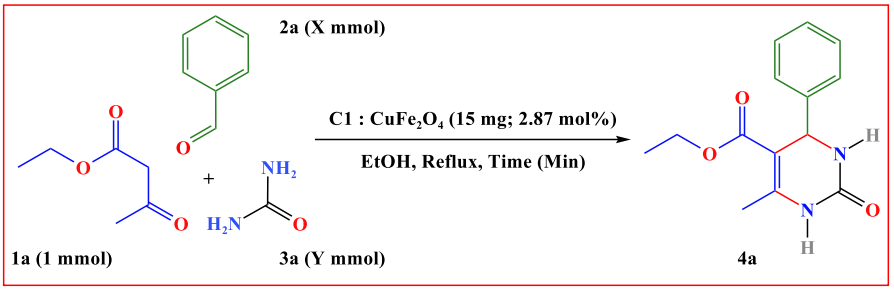

Entry	2a (mmol)	3a (mmol)	4a% Yield [b]
1	1.0	1.2	63
2	1.0	1.3	66
3	1.0	1.4	66
4	1.1	1.2	70
5	**1.1**	**1.3**	**77**
6	1.1	1.4	76
7	1.2	1.2	70
8	1.2	1.3	77
9	1.2	1.4	77

[a]1 mmol Ethyl acetoacetate, Y mmol Urea, X mmol Benzaldehyde, 5 mL Ethanol, C1-$CuFe_2O_4$ MNPs (15 mg; 2.87 mol %), for 90 min

[b]Yield that can be isolated

The best values indicates in bold

functional groups in the reactants. The manufactured nanocatalyst's Lewis acid role is crucial in facilitating the synthesis of DHPM derivatives.

Overall, the morphology of a manufactured nanocatalyst, the synergistic effects of $CuFe_2O_4$ components, its active sites, and their Lewis acid role are all interconnected aspects that substantially impact the production of DHPM derivatives.

Study of recovery and reusability of biosynthesized spinel $CuFe_2O_4$ MNPs

Following the end of the reaction, the recovered catalyst was washed five to six times with 1 mL ethanol and then dried in a hot air oven for one hour at 150 °C. The same NPs were then activated for use in further cycles by heating them to 300 °C for three hours in a muffle furnace. It is interesting to note that even after four reuses, the catalytic activity of the biosynthesized spinel $CuFe_2O_4$ MNPs

Table 6 Optimization of catalytic amount for the preparation of ethyl 1,2,3,4-tetrahydro-6-methyl-2-oxo-4-phenylpyrimidine-5-carboxylate [a]

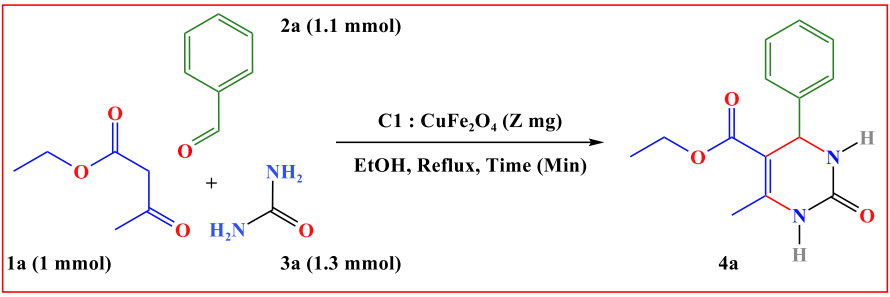

Entry	Loading of catalyst (Z mg)	Yield (4a %)[b]
1	15	14
2	20	26
3	25	41
4	30	52
5	35	69
6	40	83
7	**45**	**98**
8	50	97

[a]1.1 mmol Benzaldehyde, 1 mmol Ethyl acetoacetate, 1.3 mmol Urea, 5 mL Ethyl alcohol, Catalyst-C1-$CuFe_2O_4$ MNPs (Z mg), for 40 min

[b]Yield that can be isolated

The best values indicates in bold

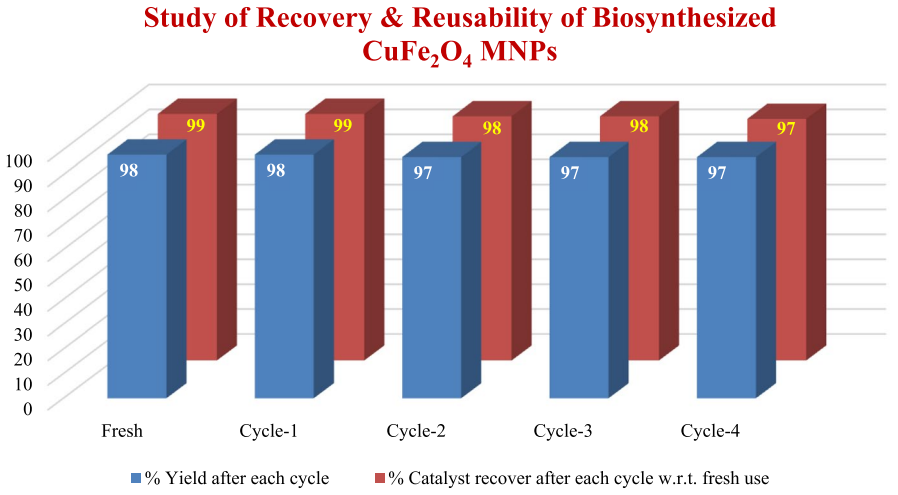

Fig. 9 Study of recovery and reusability of biosynthesized spinel $CuFe_2O_4$ MNPs as a heterogeneous catalyst for the synthesis of DHPMs under standard conditions shown in Scheme 2 (Entry 1)

Table 7 Comparative performance of the manufactured nanocatalyst in this work with previously reported catalysts for Biginelli reaction

SI. no	Catalyst	Reaction conditions	Solvent	Time	Yield (%)	References
1	Fe_3O_4@Nb_2O_5	80 ℃	Ethanol	12 h	99	[74]
2	Fe_3O_4@mesoporous SBA-15	80 °C	Ethanol	5–12 h	10–85	[75]
3	$LaCl_3{\cdot}7H_2O$/HCl	Reflux	Ethanol	5 h	96	[76]
4	Fe – Al/clay	100 °C	Solvent-free	3–5 h	86–98	[77]
5	$Bi_2Mn_2O_7$	104 °C	Solvent-free	1 h	89	[78]
6	Nb_2O_5/T	130 °C	Solvent-free	1 h	94	[79]
7	**$CuFe_2O_4$**	**Reflux**	**Ethanol**	**40 min**	**98**	**Present work**

(C1) was unaffected. For each cycle of using $CuFe_2O_4$ MNPs (C1), Fig. 9 displays the recovery and associated yield of 4a graphically. When we contrasted our present results with those of diverse previously published catalysts, we noticed that many previously reported protocols had lower yields or required longer reaction times and temperatures (Table 7).

A plausible Biginelli multicomponent cycloaddition reaction mechanism

As a result of the intermediates observed in the Biginelli reaction, three proposed mechanistic paths were reported according to various theoretical and experimental studies for the Biginelli reaction [29]. Namely, the intermediate observed in the Biginelli reaction is iminium intermediate [80], enamine intermediate [81], and chalcone (Knoevenagel route) intermediate [82]. There have been numerous comparative studies done on the Biginelli reaction mechanistic path in the past decade, such as those carried out by Puripat et al. [83], Neto et al. [84], and De Souza et al. [85]. According to their findings (AFIT and DFT calculation), Iminium salt as a reactive intermediate is preferable over Enamine and Knoevenagel intermediate [85]. In the iminium route, condensation of urea and aldehyde first takes place to get the iminium intermediate, and the applied nanocatalyst $CuFe_2O_4$ acts as a Lewis acid and activates the functional group. Further, the nucleophilic addition of enol (ethyl 3-hydroxybut-2-enoate in-situ produced from ethyl acetoacetate) results in DHPMs formation (Fig. 10).

Conclusion

Here, for the first time, we report the multicomponent Biginelli reaction using the spinel $CuFe_2O_4$ magnetic recoverable heterogeneous catalyst, synthesized via a biological route using cow milk Yogurt. The catalyst was fabricated through a green method and then analyzed using XRD, FESEM, EDX, UV-DRS, FT-IR, and VSM techniques. Furthermore, the synthesis of ethyl

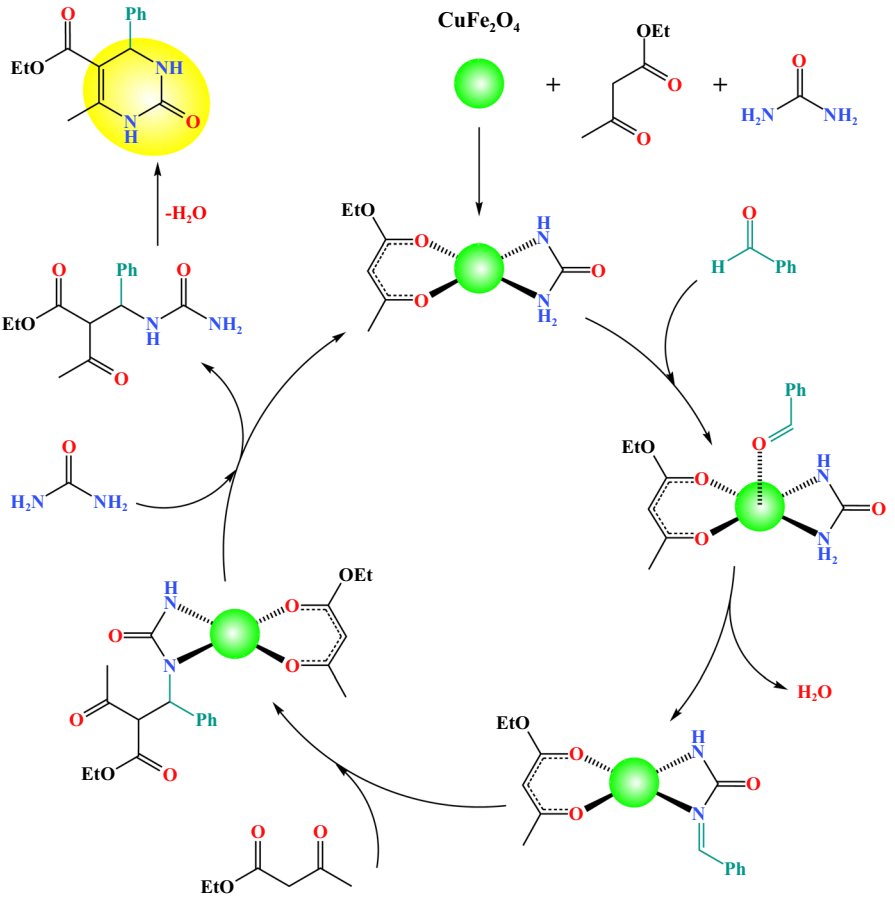

Fig. 10 Possible reaction mechanism of spinel $CuFe_2O_4$ MNPs catalyzed synthesis of ethyl 1,2,3,4-tetrahydro-6-methyl-2-oxo-4-arylpyrimidine-5-carboxylate derivative

1,2,3,4-tetrahydro-6-methyl-2-oxo-4-arylpyrimidine-5-carboxylate derivative (4a-4i) with excellent yields of products/ derivatives was completed using an ethyl acetoacetate with several substituted aromatic carbaldehydes, urea and a catalytic amount of magnetically separable spinel $CuFe_2O_4$ nanomaterial in ethyl alcohol as a reaction medium. This protocol's major benefits include a simple reaction workup process, cleanliness and safety, and enormous yields of final products. This bio-inspired synthesis of spinel $CuFe_2O_4$ MNPs may expose new aspects for discovering their conceivable role in organic synthesis and conversion.

Supplementary Information The online version contains supplementary material available at https://doi.org/10.1007/s11164-024-05322-5.

Acknowledgements We gratefully thank SAIF Punjab for ^{1}H and ^{13}C NMR analysis.

Authors' contributions Dnyaneshwar Sanap involved in conceptualization, investigation, data curation, writing—original draft. Lata Avhad involved in data curation, writing—original draft. Satish Ahire involved in data curation. Mahmoud Mirzaei and Deepak Kumar involved in visualization, supervison. Suresh Ghotekar involved in conceptualization, investigation, supervison, writing—original draft. Nitin D. Gaikwad involved in writing—review and editing, supervison.

Funding Not applicable.

Data availability Data will be made available on request.

Declarations

Conflict of interests The authors declare no conflict of interest.

Ethical approval Not applicable.

References

1. G. Sharma, A. Kumar, S. Sharma, M. Naushad, R.P. Dwivedi, Z.A.L. Othman, G. Mola, J. King Saud Univ. Sci. **31**, 257–269 (2019)
2. R. Eivazzadeh-Keihan, H. Bahreinizad, Z. Amiri, H.A.M. Aliabadi, M. Salimi-Bani, A. Nakisa, F. Davoodi, B. Tahmasebi, F. Ahmadpour, F. Radinekiyan, TrAC, Trends Anal. Chem. **141**, 116291 (2021)
3. H.N. Cuong, S. Pansambal, S. Ghotekar, R. Oza, N.T.T. Hai, N.M. Viet, V.-H. Nguyen, Environ. Res. **203**, 111858 (2022)
4. D. Astruc, Chem. Rev. **120**, 461–463 (2020)
5. L.J. Berchmans, R.K. Selvan, C. Augustin, Mater. Lett.Lett. **58**(12–13), 1928–1933 (2004)
6. A. Bigdeli, F. Ghasemi, H. Golmohammadi, S. Abbasi-Moayed, M.A.F. Nejad, N. Fahimi-Kashani, S. Jafarinejad, M. Shahrajabian, M.R. Hormozi-Nezhad, Nanoscale **9**(43), 16546–16563 (2017)
7. K. An, G.A. Somorjai, Catal. Lett. **145**, 233–248 (2015)
8. S. Ghotekar, D. Sanap, K.-Y.A. Lin, H. Louis, D. Pore, R. Oza, Res. Chem. Intermed. **50**(1), 49–68 (2024)
9. P. Pharande, G. Rashinkar, S. Ghotekar, D. Pore, Res. Chem. Intermed. **49**(6), 2433–2453 (2023)
10. R. Eivazzadeh-Keihan, H.A.M. Aliabadi, F. Radinekiyan, M. Sobhani, A. Maleki, H. Madanchi, M. Mahdavi, A.E. Shalan, RSC Adv. **11**(29), 17914–17923 (2021)
11. R. Eivazzadeh-Keihan, F. Khalili, N. Khosropour, H.A.M. Aliabadi, F. Radinekiyan, S. Sukhtezari, A. Maleki, H. Madanchi, M.R. Hamblin, M. Mahdavi, A.C.S. Appl, Mater. Interfaces **13**(29), 33840–33849 (2021)
12. A. Shaabani, A. Maleki, Chem. Pharm. Bull. **56**(1), 79–81 (2008)
13. R. Soni, A. Thakur, S. Ghotekar, P. Lokhande, R. Aepuru, S. Manda, D. Kumar, N.M. Mubarak, J. Alloys Compd. **993**, 174542 (2024)
14. Y. Fu, Q. Chen, M. He, Y. Wan, X. Sun, H. Xia, X. Wang, Ind. Eng. Chem. Res. **51**(36), 11700–11709 (2012)
15. K. Elayakumar, A. Manikandan, A. Dinesh, K. Thanrasu, K.K. Raja, R.T. Kumar, Y. Slimani, S. Jaganathan, A. Baykal, J. Magn. Magn. Mater. **478**, 140–147 (2019)
16. M.A. Haija, A.F. Abu-Hani, N. Hamdan, S. Stephen, A.I. Ayesh, J. Alloys Compd. **690**, 461–468 (2017)
17. S. Keerthana, R. Yuvakkumar, G. Ravi, S. Pavithra, M. Thambidurai, C. Dang, D. Velauthapillai, Environ. Res. **200**, 111528 (2021)
18. R. Li, M. Cai, Z. Xie, Q. Zhang, Y. Zeng, H. Liu, G. Liu, W. Lv, Appl. Catal. B Environ. **244**, 974–982 (2019)
19. S. Anandan, T. Selvamani, G.G. Prasad, A. Asiri, J. Wu, J. Magn. Magn. Mater. **432**, 437–443 (2017)
20. R. Parella, S.A. Babu, Catal. Commun. **29**, 118–121 (2012)

21. N.-K. Nguyen, M.-T. Ha, H.Y. Bui, Q.T. Trinh, B.N. Tran, T.Q. Hung, T.T. Dang, X.H. Vu, Catal. Commun. **149**, 106240 (2021)
22. M.A.E.A.A.A. El-Remaily, A.M. Abu-Dief, Tetrahedron **71**(17), 5279–2584 (2015)
23. A. Maleki, Helv. Chim. Acta **97**(4), 587–593 (2014)
24. T. Amuthan, R. Sanjeevi, G. Kannan, A. Sridevi, Phys. B: Condens. Matter **638**, 413842 (2022)
25. H. Hou, G. Xu, S. Tan, Y. Zhu, Infrared Phys. Technol. **85**, 261–265 (2017)
26. J. Kurian, M.J. Mathew, J. Magn. Magn. Mater. **451**, 121–130 (2018)
27. S. Tajik, H. Beitollahi, Food Chem. Toxicol. **165**, 113048 (2022)
28. P.S.M. Kumar, A.P. Francis, T. Devasena, J. Environ. Nanotechnol. **3**(3), 73–81 (2014)
29. D. Sanap, L. Avhad, S. Ghotekar, N.D. Gaikwad, J. Mol. Struct.Struct. **1283**, 135246 (2023)
30. S. Ghotekar, P. Basnet, K.-Y.A. Lin, A. Rahdar, A.P. Larios, V. Gandhi, R. Oza, J. Sol-Gel Sci. Technol. **106**(3), 726–736 (2023)
31. S. Pansambal, R. Oza, S. Borgave, A. Chauhan, P. Bardapurkar, S. Vyas, S. Ghotekar, Appl. Nanosci. **13**(9), 6067–6092 (2023)
32. S. Sharma, P. Jakhar, H. Sharma, J. Chin. Chem. Soc. **70**(2), 107–127 (2023)
33. V. Aswathi, S. Meera, C.A. Maria, M. Nidhin, Nanotechnol. Environ. Eng. **2022**, 1–21 (2022)
34. Y. Zhang, Y. Chen, Z.-W. Kang, X. Gao, X. Zeng, M. Liu, D.-P. Yang, Colloids Surf A Physicochem Eng AspPhysicochem. Eng. Asp. **612**, 125874 (2021)
35. N.J. Vickers, Curr. Biol. **27**(14), R713–R715 (2017)
36. P. Kumar, H. Mishra, Food Bioprod. Process. **82**(2), 133–142 (2004)
37. F.S. Vianna, A.C.V.D.C.S. Canto, B. Costa-Lima, A.P. Salim, C.F. Balthazar, M.P. Costa, P. Panzenhagen, R. Rachid, R.M. Franco, C. Adam Conte-Junior, Cienc. Rural Rural **49**, e20180522 (2019)
38. G.K. Deshwal, S. Tiwari, A. Kumar, R.K. Raman, S. Kadyan, Trends Food Sci. Technol. **109**, 499–512 (2021)
39. R.K. Ganta, A. Ramgopal, C. Ramesh, K.R. Babu, M.M. Krishna Kumar, B.V. Rao, Synth. Commun.Commun. **46**(24), 1999–2008 (2016)
40. P.D. Sanasi, D. Santhipriya, Y. Ramesh, M.R. Kumar, B. Swathi, K.J. Rao, J. Chem. Sci. **126**, 1715–1720 (2014)
41. S. Bandaru, R.B. Korupolu, P.D. Sanasi, IOSR J. Appl. Chem. **11**, 28–37 (2018)
42. A.H. Cahyana, A.R. Liandi, Y. Yulizar, Y. Romdoni, T.P. Wendari, Ceram. Int. **47**(15), 21373–21380 (2021)
43. K. De, S. Chandra, B. Sarkar, S. Ganguly, M. Misra, J. Radioanal. Nucl. Chem. **283**, 621–628 (2010)
44. I.-T. Crevel, M. Alonso, R. Cross, Curr. Biol. **14**(11), R411–R412 (2004)
45. S.H. Choi, D. McCollum, Curr. Biol. **22**(3), 225–230 (2012)
46. J.C. Cochran, S.P. Gilbert, Biochem. **44**(50), 16633–16648 (2005)
47. S. DeBonis, J.-P. Simorre, I. Crevel, L. Lebeau, D.A. Skoufias, A. Blangy, C. Ebel, P. Gans, R. Cross, D.D. Hackney, Biochem. **42**(2), 338–349 (2003)
48. K. Drosopoulos, C. Tang, W.C. Chao, S. Linardopoulos, Nat. Commun. **5**(1), 3686 (2014)
49. A.N. de Fatima, T.C. Braga, L.D.S. Neto, B.S. Terra, B.G. Oliveira, D.L. da Silva, L.V. Modolo, J. Adv. Res. **6**(3), 363–373 (2015)
50. N. Janković, J.T. Ristovski, M. Vraneš, A. Tot, J. Petronijević, N. Joksimović, T. Stanojković, M.Đ Crnogorac, N. Petrović, I. Boljević, Bioinorg. Chem. **86**, 569–582 (2019)
51. C.O. Kappe, Eur. J. Med. Chem. **35**(12), 1043–1052 (2000)
52. L.H.S. Matos, F.T. Masson, L.A. Simeoni, M. Homem-de-Mello, Eur. J. Med. Chem. **143**, 1779–1789 (2018)
53. A. Paraskar, G. Dewkar, A. Sudalai, Tetrahedron Lett. **44**(16), 3305–3308 (2003)
54. K.A. Kumar, M. Kasthuraiah, C.S. Reddy, C.D. Reddy, Tetrahedron Lett. **42**(44), 7873–7875 (2001)
55. I. Suzuki, Y. Suzumura, K. Takeda, Tetrahedron Lett. **47**(45), 7861–7864 (2006)
56. S.-Y. Zhao, Z.-Y. Chen, N. Wei, L. Liu, Z.-B. Han, Inorg. Chem. **58**(12), 7657–7661 (2019)
57. A. Shaabani, E. Soleimani, A. Maleki, J. Moghimi-Rad, Synth. Commun. **38**(7), 1090–1095 (2008)
58. P. Pharande, P. Mhaldar, T. Lohar, S. Ghotekar, T.N. Chhowala, G. Rashinkar, D. Pore, Res. Chem. Intermed. **49**(10), 4541–4560 (2023)
59. D. Sanap, L. Avhad, S. Ghotekar, N.D. Gaikwad, Inorg. Chem. Commun. **149**, 110387 (2023)
60. S. Ghotekar, D. Sanap, K. Patel, Y. Abhale, A. Chauhan, L. Li, D. Kumar, K.-Y.A. Lin, R. Oza, Res. Chem. Intermed. **2024**, 1–21 (2024)
61. J. Safari, S. Gandomi-Ravandi, J. Mol. Catal. A Chem. **373**, 72–77 (2013)

62. J. SafaeiGhomi, R. Teymuri, A. Ziarati, Monatsh Fur Chem. **144**, 1865–1870 (2013)
63. Z. Varzi, A. Maleki, Appl. Organomet. Chem. **33**(8), e5008 (2019)
64. S. Prakash, N. Elavarasan, A. Venkatesan, K. Subashini, M. Sowndharya, V. Sujatha, Adv. Powder Technol. **29**(12), 3315–3326 (2018)
65. F. Zamani, E. Izadi, Catal. Commun. **42**, 104–108 (2013)
66. D. Girija, H.B. Naik, B.V. Kumar, C. Sudhamani, K. Harish, Arab. J. Chem. **12**(3), 420–428 (2019)
67. G.R. Chaudhary, P. Bansal, S. Mehta, Chem. Eng. J. **243**, 217–224 (2014)
68. E. Prince, R. Treuting, Acta Crystallogr. **9**(12), 1025–1028 (1956)
69. K. Kombaiah, J.J. Vijaya, L.J. Kennedy, M. Bououdina, Ceram. Int. **42**(2), 2741–2749 (2016)
70. A. Phuruangrat, B. Kuntalue, S. Thongtem, T. Thongtem, Mater. Lett. **167**, 65–68 (2016)
71. J. Kurian, M.J. Mathew, J. Magn. Magn. Mater. **428**, 204–212 (2017)
72. M. Satheeshkumar, E.R. Kumar, C. Srinivas, G. Prasad, S.S. Meena, I. Pradeep, N. Suriyanarayanan, D. Sastry, J. Magn. Magn. Mater. **484**, 120–125 (2019)
73. A. Al-Hunaiti, N. Al-Said, L. Halawani, M.A. Haija, R. Baqaien, D. Taher, Arab. J. Chem. **13**(4), 4945–4953 (2020)
74. C.G. Lima, S. Silva, R.H. Goncalves, E.R. Leite, R.S. Schwab, A.G. Correa, M.W. Paixao, ChemCatChem **6**(12), 3455–3463 (2014)
75. J. Mondal, T. Sen, A. Bhaumik, Dalton Trans. **41**(20), 6173–6181 (2012)
76. J. Lu, Y. Bai, Z. Wang, B. Yang, H. Ma, Tetrahedron Lett. **41**(47), 9075–9078 (2000)
77. B.A. Dar, P. Patidar, S. Kumar, M.A. Wagay, A.K. Sahoo, P.R. Sharma, S. Pandey, M. Sharma, B. Singh, J. Chem. Sci. **125**, 545–553 (2013)
78. S. Khademinia, M. Behzad, A. Alemi, M. Dolatyari, S.M. Sajjadi, RSC Adv. **5**(87), 71109–71114 (2015)
79. L.G. do Nascimento, I.M. Dias, G.B. de Meireles Souza, I. Dancini-Pontes, N.R.C. Fernandes, P.S. de Souza, G. de Roberto Oliveira, C.G. Alonso, J. Org. Chem. **85**(17), 11170–11180 (2020)
80. C.O. Kappe, J. Org. Chem. **62**(21), 7201–7204 (1997)
81. K. Folkers, T.B. Johnson, J. Am. Chem. Soc. **55**(9), 3784–3791 (1933)
82. F. Sweet, J.D. Fissekis, J. Am. Chem. Soc. **95**(26), 8741–8749 (1973)
83. M. Puripat, R. Ramozzi, M. Hatanaka, W. Parasuk, V. Parasuk, K. Morokuma, J. Org. Chem. **80**(14), 6959–6967 (2015)
84. L.M. Ramos, A.Y. de Ponce Leon y Tobio, M.R. dos Santos, H.C. de Oliveira, A.F. Gomes, F.C. Gozzo, A.L. de Oliveira, B.A. Neto, J. Org. Chem. **77**(22), 10184–10193 (2012)

85. R.O. De Souza, E.T. da Penha, H.M. Milagre, S.J. Garden, P.M. Esteves, M.N. Eberlin, O.A. Antunes, Chem. Eur. J. **15**(38), 9799–9804 (2009)

Authors and Affiliations

Dnyaneshwar Sanap[1,2] · Lata Avhad[3] · Satish Ahire[4] · Mahmoud Mirzaei[5] · Deepak Kumar[6] · Suresh Ghotekar[7] · Nitin D. Gaikwad[1]

✉ Dnyaneshwar Sanap
sanapdnyanu90258@gmail.com

✉ Suresh Ghotekar
ghotekarsuresh7@gmail.com

Nitin D. Gaikwad
gaikwad_nd17@yahoo.co.in

1 Department of Chemistry, Organic Chemistry Research Centre, K.R.T. Arts, B.H. Commerce, and A.M. Science College, Savitribai Phule Pune University, Gangapur Road, Nashik, Maharashtra 422002, India

2 Department of Chemistry, KPG Arts, Commerce, and Science College, Savitribai Phule Pune University, Igatpuri, Maharashtra 422403, India

3 Department of Chemistry, Organic Chemistry Research Centre, Karmaveer Shantarambapu Kondaji Wavare Arts, Science and Commerce College, CIDCO, Savitribai Phule Pune University, Uttamnagar, Nashik, Maharashtra 422008, India

4 Department of Chemistry, Maharaja Sayajirao Gaikwad Arts, Science and Commerce College, Savitribai Phule Pune University, Malegaon Camp, Malegaon, Maharashtra,, India

5 Department of Natural and Mathematical Sciences, Faculty of Engineering, Tarsus University, Tarsus, Turkey

6 Department of Chemistry, School of Chemical Engineering and Physical Sciences, Lovely Professional University, Phagwara, Punjab 144411, India

7 Centre for Herbal Pharmacology and Environmental Sustainability, Chettinad Hospital and Research Institute, Chettinad Academy of Research and Education, Kelambakkam, Tamil Nadu 603103, India